Christ Journal of Science
www.christcollegerajkot.edu.in
ISSN: 3139-0951 (Online)
Vol 2/Issue1/ January--June/2026

REVIEW ARTICLE ON CHARACTERIZATION OF Na_2S DOPED ADP CRYSTALS

A.P. Kochuparampil and S.J. Shah
Physics Department, Christ College, Rajkot, Gujarat
Corresponding Author's Email: prasadashish7963@gmail.com

Abstract

Ammonium dihydrogen phosphate (ADP) is an important inorganic crystal with significant applications in nonlinear optics, electro-optics, acousto-optics, and related photonic devices. The present review focuses on the growth and comprehensive characterization of di-sodium sulphide (Na_2S)-added ADP crystals and examines the influence of Na_2S incorporation on their structural, spectroscopic, thermal, dielectric, electrical, impedance, and nonlinear optical properties. Na_2S nanoparticles were synthesized using a co-precipitation method followed by microwave irradiation, and transmission electron microscopy revealed nearly spherical nanoparticles with sizes ranging from approximately 9 to 20 nm. Pure and Na_2S-added ADP crystals were subsequently grown by the slow solvent evaporation technique. Powder X-ray diffraction studies confirmed the single-phase tetragonal nature of the crystals, while peak shifts and variations in lattice parameters indicated successful incorporation of the dopant. Atomic absorption spectroscopy and FTIR analysis further supported the presence of Na and sulphur-related modifications within the ADP lattice. Thermal analysis revealed a marginal reduction in thermal stability for Na_2S-added crystals compared with pure ADP. Dielectric constant, dielectric loss, and AC conductivity studies demonstrated significant modifications in electrical behaviour upon Na_2S addition. Impedance and modulus spectroscopic analyses revealed changes in grain and grain-boundary contributions and confirmed non-Debye relaxation behaviour. The nonlinear optical investigation demonstrated a substantial enhancement in second harmonic generation efficiency for Na_2S-added ADP crystals. Among the investigated samples, the 5NADP crystal exhibited the highest electro-optic coefficient, polarizability, and SHG efficiency, indicating its superior nonlinear optical performance. Overall, Na_2S addition effectively modifies the physicochemical and optical characteristics of ADP crystals, highlighting their potential for improved nonlinear optical and photonic applications.

Keywords: Ammonium dihydrogen phosphate; ADP crystals; Na_2S nanoparticles; crystal growth; dielectric properties; impedance spectroscopy; nonlinear optics; second harmonic generation.

Introduction:

Ammonium dihydrogen phosphate (ADP) is a technologically very important inorganic crystal. It is used and studied widely as one of the primary materials for its nonlinear optical, electro-optical, acoustic-optical, phase matching, optical mixing and anti-ferroelectric properties [1–5]. These properties are extensively explored for various ADP-based device applications [6]. In a recent study, the third harmonic generation (THG) efficiency of ADP has been evaluated and it is found to be 50% higher than KDP, therefore, ADP is suggested as an alternative of the KDP crystal in the inertial confinement of fusion experiments [7].

Furthermore, there have been various synthesis techniques that have caught equal attention of researchers and industrialists alike. Below is the list of various such techniques that have been frequently used for the synthesis of such crystals.

Crystal growth methods are broadly categorized by the nutrient phase (melt, solution, vapor, or solid) and the various involved techniques are

- Czochralski (melt pulling)
- Bridgman (melt solidification)
- Floating Zone (melt zone)
- Hydrothermal (solution under high temp/pressure)
- Solvent Evaporation (solution cooling/evaporation)

ISSN: 3139-0951 (Online)
Vol 2/Issue1/ January--June/2026

- Vapor Phase Transport (PVT/CVT),

Which all are aiming to form high-quality single crystals for electronics, optics and research.

1. Melt Growth Methods (Liquid to Solid)

They are popular for formation of large, high-purity single crystals like semiconductors.

- Czochralski (CZ) Method: Pulls a seed crystal from a molten material, creating large cylindrical boules (e.g., silicon).
- Bridgman-Stockbarger Method: A crucible with melt is slowly moved through a furnace, solidifying from one end.
- Floating Zone (FZ) Method: A molten zone is moved along a solid rod, purifying and growing the crystal (e.g., high-purity silicon).
- Heat Exchange Method (HEM): Solidification occurs from the bottom up, controlled by a heat exchanger.

2. Solution Growth Methods (Solution to Solid)

Used for materials that decompose before melting or require high purity.

- Solvent Evaporation: Cooling or evaporating a solvent from a saturated solution (e.g., sugar, salt).
- Hydrothermal Synthesis: Growing crystals from aqueous solutions under high temperature and pressure (e.g., quartz).
- Flux Growth: Using a high-temperature solvent (flux) that remains liquid to dissolve the material (e.g., garnets, high-Tc superconductors).
- Gel Growth: Crystals grow within a porous gel medium, offering slow, controlled growth and low defects.

3. Vapor Phase Growth Methods (Vapor to Solid)

Ideal for complex materials and thin films.

- Physical Vapor Transport (PVT): Material sublimates and deposits onto a cooler substrate (e.g., SiC).
- Chemical Vapor Deposition (CVD): Chemical reactions on a heated substrate form the crystal.
- Epitaxy: Growing a thin layer of crystal on a single-crystal substrate (e.g., GaN on Sapphire).

4. Solid Phase Growth (Solid to Solid)

Used for materials that don't melt or dissolve easily, often involving solid-state reactions or recrystallization.

- Solid-State Recrystallization: High-temperature annealing of polycrystalline material to form larger grains.
- Hot Pressing/Sintering: Applying heat and pressure to consolidate powders.

5. Other Techniques are

- Verneuil (Flame Fusion) Method: Dropping powder through an oxyhydrogen flame to form single crystals (e.g., ruby, sapphire).
- Laser-Heated Pedestal Growth (LHPG): Uses a laser to melt the tip of a rod, growing a crystal from the melt (e.g., fibers).

To engineer and modify the properties of the ADP crystals, several amino acids have been doped in ADP crystals in the author's laboratory and characterized extensively [8–12]. Apart from this, an attempt has been made to dope Sr^{2+} in ADP crystal and study their linear and nonlinear optical, dielectric and impedance properties [13]. Recently, a detailed review on KDP and ADP crystals has been published [14]. Earlier, only two reports are available on addition of chalcogenide nanoparticles ZnS and CdS in ADP crystals [15,16]. In the current article, the author cites the investigation on pure and chalcogenide compound di-sodium sulphide (Na_2S) nanoparticles added ADP crystals.

In the current article, we used the co-precipitation technique as it was found suitable and convenient as per the expertise of our group and the availability of resources.

Experimental techniques:

Synthesis of di-sodium sulphide compound:

Di-sodium sulphide (Na_2S) was synthesised by co-precipitation method and then the sample was irradiated through microwave irradiation. The 0.5M sodium acetate (CH_3COONa) and 1.5M thiourea (CH_4N_2S) solutions were taken as starting materials. The solution of sodium acetate was filled in burette. The 10ml capping agent ethylene diamine was added in the thiourea

ISSN: 3139-0951 (Online)
Vol 2/Issue1/ January--June/2026

solution and heated at 70^{0}C. The solution of sodium acetate was added in drop-wise manner into the thiourea solution, resulting towards light yellowish precipitates in colloidal form. After continuous stirring of 7 hours the colloidal solution was subjected to the microwave irradiation in domestic microwave oven of Kenstar having input power of 1450W and by adjusting the microwave irradiation 10% of input power, i.e. 145W, for 15 minutes till that the solution completely evaporated and only solid remained which was further washed by distilled water and acetone. The dried irradiated sample was crushed using mortar pestle. As the chalcogenide compound Na_2S is moderately soluble in water (18.6g /100 ml at 20 ^{0}C and 39g /100 ml at 50 ^{0}C). In order to increase the solubility of Na_2S nano-particles, ethylene diamine is used as a dispersing agent. The solubility of Na_2S nanoparticles was found to be 18.7 g/100ml, which is increased by 0.18g/100ml compared to the bulk Na_2S (18.6g/100ml).

TEM was performed to check for the morphology of the crystal and the results obtained are discussed here. The TEM image shown in Figure (1) indicates nano-particles with spherical morphology and particle size within 9 nm to 20 nm. They are observed to lie within the expected range and suggest nanostructure formation.

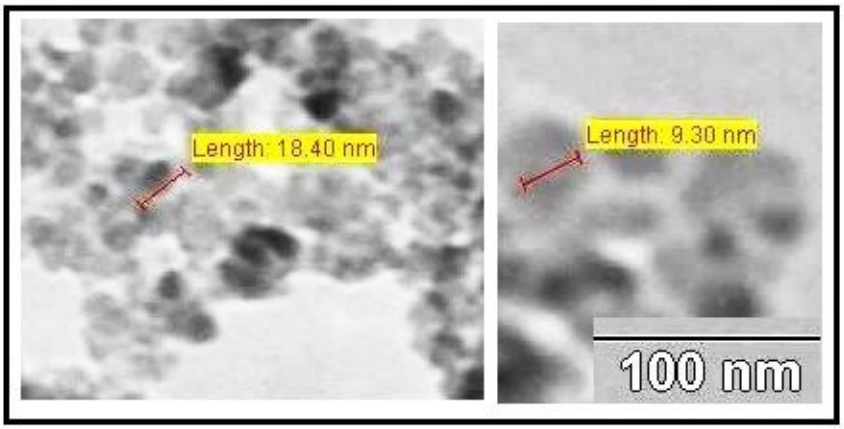


Figure (1): TEM image of di-sodium sulphide nano-particles

Crystal growth:

Pure ADP and Na_2S added ADP crystals were grown by using the slow solvent evaporation method at room temperature. Required amount of ADP (184 g) was added to 400ml distilled water under constant stirring to achieve saturation. After rigorous stirring for 4 hours, the solution was filtered using Watmann filter paper no.1. Then the solution was sub-divided into four beakers; one beaker contains 100ml pure ADP solution and in the other three beakers, 2ml, 5ml and 10ml Na_2S solutions were added in ADP solutions and stirred for 3 hours. The samples were labelled as 2NADP, 5NADP and 10NADP for 2ml, 5ml and 10ml Na_2S solutions added ADP, respectively. After 15 days, the highly transparent and good quality crystals have been grown. Due to the doping of Na_2S in ADP crystals, no colour change was observed, but the change in morphology indicated the presence of dopants in ADP crystals as shown in Figure (2).

The change in morphology indicates the successful incorporation of the dopants because dopants likely to alter the growth rates of different faces in different manner. Figure (3) shows the schematic diagram of the growth process adopted.

ISSN: 3139-0951 (Online)
Vol 2/Issue1/ January--June/2026

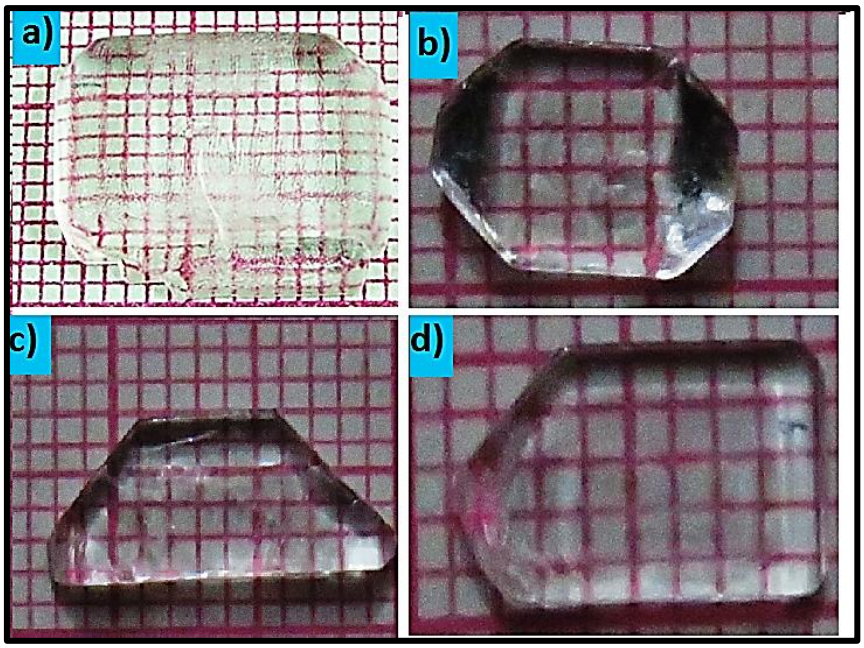


Figure (2): a) Pure ADP, b) 2NADP, c) 5NADP and d) 10NADP

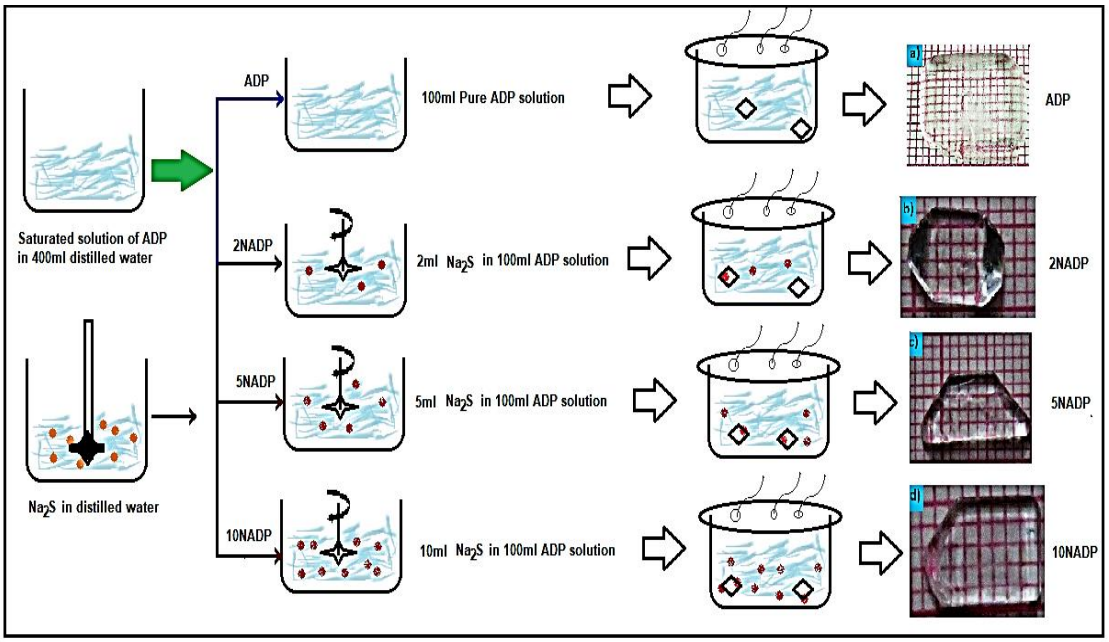


Figure (3): Schematic diagram of the crystal growth process

Powder XRD:

Figure (4) shows the powder XRD patterns of pure and Na_2S added ADP crystals. It is clear from the patterns that all Na_2S added ADP crystals possess single phase nature. However, the peak shifting and peak intensity changes are observed indicating the presence of the dopants. This is shown by figure (5) indicating the (101), (200) and (112) peaks in the XRD pattern of figure (4) in the expanded scale. With comparison to pure ADP, the peak broadening decreases for Na_2S added ADP crystals which further suggests that the peak intensity becomes very sharp and hence the dopant improves the crystallinity. In addition to this, marginal change in strain has been observed. Whereas, the shifting of peak is very minor towards higher angle side in all Na_2S added ADP crystals.

ISSN: 3139-0951 (Online)
Vol 2/Issue1/ January--June/2026

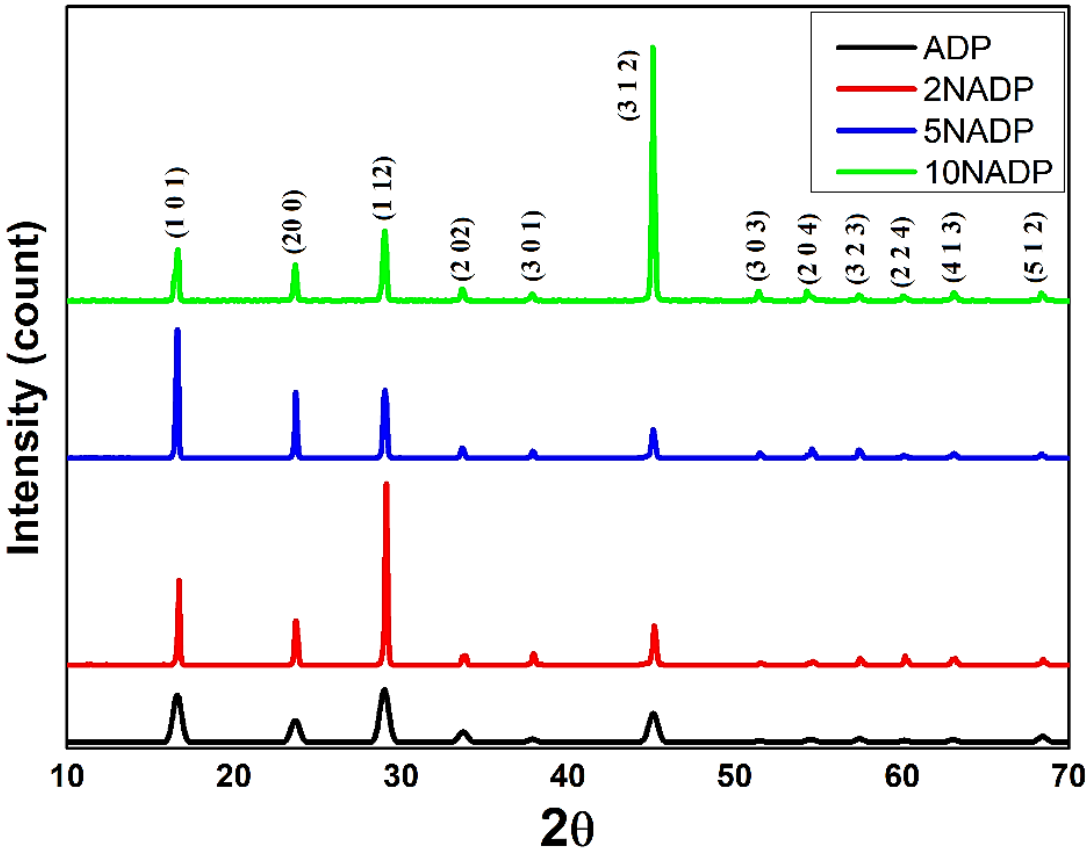


Figure (4): Powder XRD patterns of pure and Na_2S added ADP crystals

The lattice parameters of pure ADP matches with the reported values [10,15–17]. The unit cell parameters of pure and Na_2S added ADP crystals are listed in table 1.

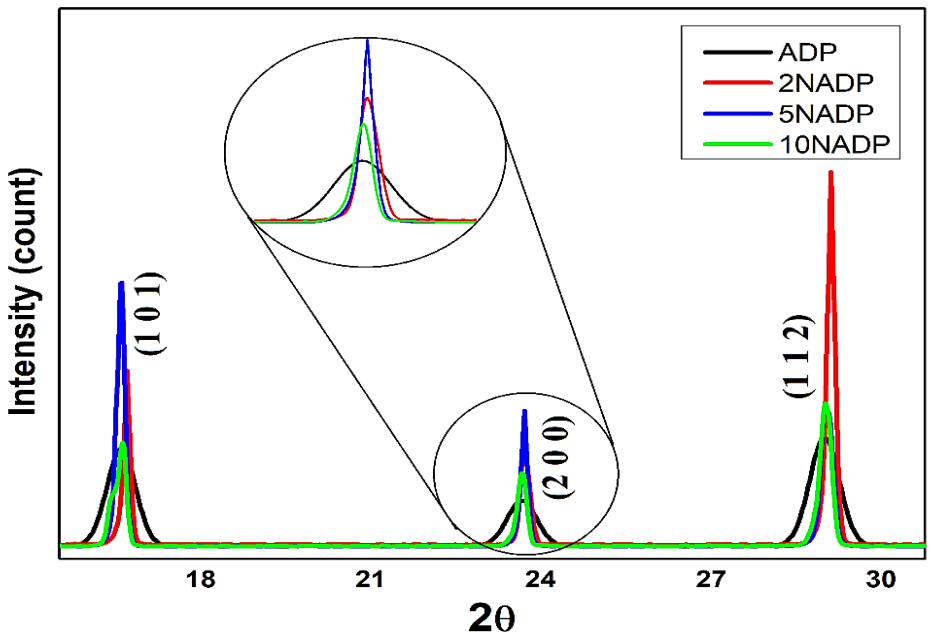


Figure (5): Powder XRD pattern on expanded scale indicating shifting of XRD peaks

ISSN: 3139-0951 (Online)
Vol 2/Issue1/ January--June/2026

Table 1: Crystal unit cell parameters and AAS data

Samples	a(Å)	b(Å)	c(Å)	Unit cell Volume(Å^3)	ppm of Na^+	Strain x 10^{-3}
ADP	7.502	7.502	7.548	424.80	-	0.70
2NADP	7.492	7.492	7.542	423.33	0.89	0.72
5NADP	7.504	7.504	7.562	425.81	1.98	0.71
10NADP	7.506	7.506	7.560	425.93	3.66	0.70

The unit cell volume also changes on addition of Na_2S which indicates the successful inclusion of Na_2S in ADP lattice and producing the slight distortion in the lattice.

AAS study:

The AAS study was carried out for all the Na_2S added ADP crystals to find the presence of metal ion Na^+ in doped ADP crystals. The presence of Na^+ metal ions in the ADP crystals is estimated and listed in table 1.

FT-IR spectroscopy:

Figure (6) shows the FTIR spectra of pure and di-sodium sulphide added ADP crystals. The absorption band at 3100-3150 cm^{-1} is due to the O-H stretching of water. The absorption at 2370-2380 cm^{-1} is due to the stretching of the hydrogen bond. The absorption at 1400-1390 cm^{-1} is due to the bending vibration of ammonium and the absorption at 1290-1295 cm^{-1} is due to the asymmetry stretching of PO_4. The 1080-1110 cm^{-1} and 910-940 cm^{-1} show absorption due to P-O-H stretching. The absorptions at 530-540 cm^{-1} and 480-490 cm^{-1} are due to the symmetry stretching of PO_4. The spectrum obtained for the pure ADP corresponds to that reported in the literature [18]. The observed absorption and their assignments are presented in table 2.

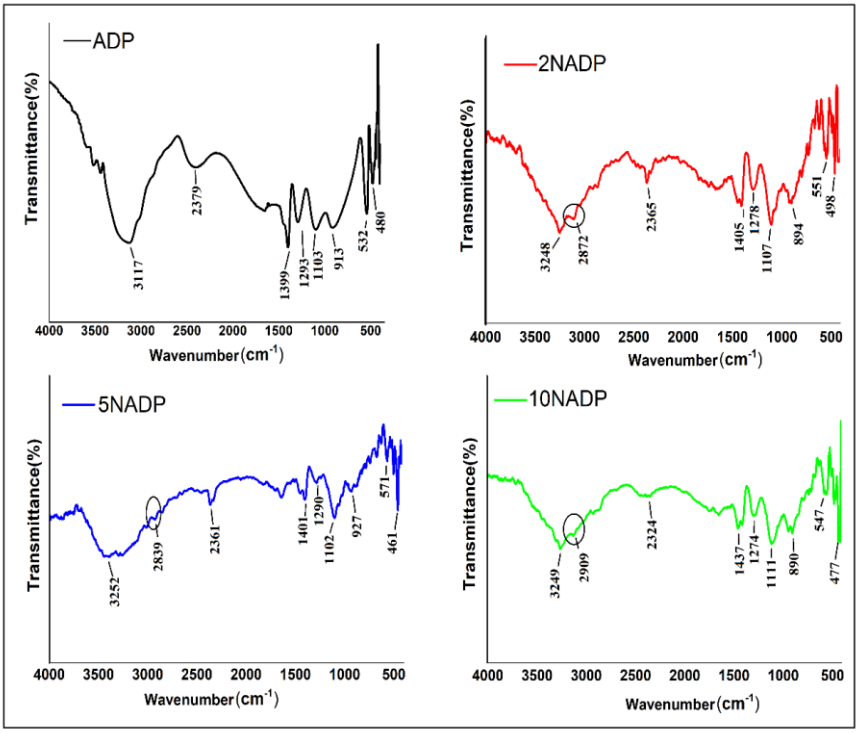


Figure (6): FT-IR spectra of pure and Na_2S added ADP

ISSN: 3139-0951 (Online)
Vol 2/Issue1/ January--June/2026

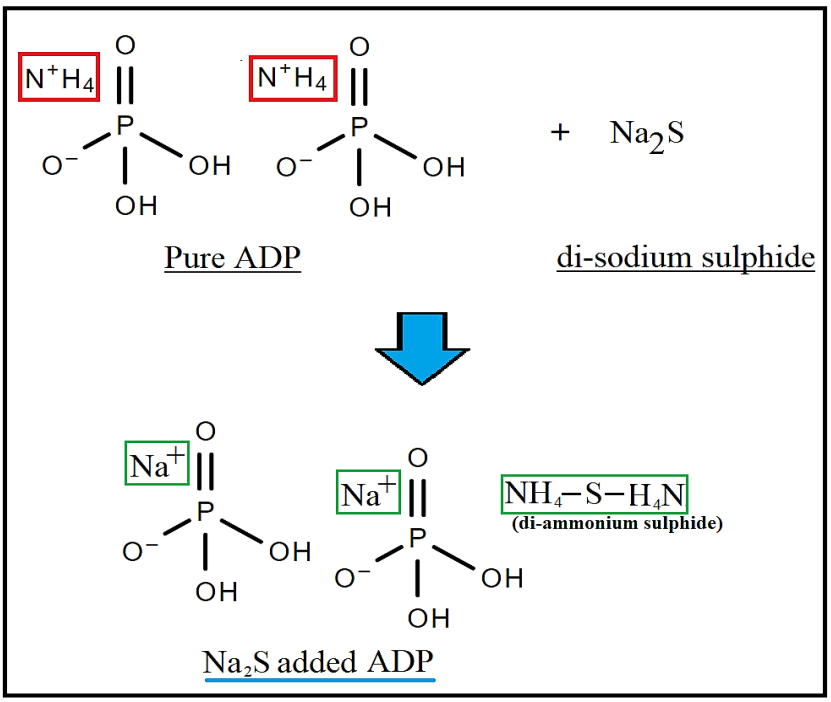


Figure (7): Tentative arrangement of molecules

Table 2: FT-IR Assignments

Wavenumber (cm^{-1})				Assignments
ADP	**2NADP**	**5NADP**	**10NADP**	
3117	3248	3252	3249	O-H stretching
-	2872	2893	2909	S-H asymmetric stretching
2379	2365	2361	2324	Stretching of hydrogen bond
1399	1405	1401	1437	Bending vibration of NH_4
1293	1278	1290	1274	Asymmetry stretching of PO_4
1103	1107	1102	1111	P-O-H stretching
913	894	927	890	P-O-H stretching
532	551	571	547	PO_4 stretching
480	498	461	477	PO_4 stretching

The shifting of absorption peaks are observed in all Na_2S added ADP samples compared to pure ADP, which indicates the partial substitution of sodium ion with ammonia ion, this may be due to the addition of Na_2S in ADP samples. Moreover, the additional absorption peaks observed in samples 2NADP, 5NADP and 10NADP at 2872 cm^{-1}, 2893 $cm^{-1}$and 2909 cm^{-1}, respectively, are assigned as S-H stretching vibration due the presence of sulphur only in Na_2S added ADP crystals. The replacement of a mono-valent ion by the other mono-valent ion may be quite simple in terms of charge balancing. From this discussion, the present author proposes a hypothesis that the NH_4^+ ion of ADP is partially replaced by sodium ion and in that process, the two ammonium ions may be reacting with sulphur and the formation of di-ammonium sulphide giving rise to S-H vibration in the FTIR spectra of Na_2S added ADP crystals. This will be again discussed in detail in Chapter IV. This is shown in the schematic diagram of figure (7). The AAS data of table 1 and the assignments of

ISSN: 3139-0951 (Online)
Vol 2/Issue1/ January--June/2026

FTIR spectra in table 2 suggest the successful addition of Na_2S in ADP crystals.

Thermal analysis:

Figure (8) exhibits slow decomposition of pure ADP with the reduction of 5% of its original weight at 280^{0}C and remains stable up to 180^{0}C. An endothermic reaction occurs at 214^{0}C, indicates the melting of a substance, which is in good agreement with the reported values in the literature [15,16,19].

In the first stage of decomposition, removal of ammonia occurs in between 150^{0}C to 245^{0}C and phosphoric acid is formed. Small exothermic peak at 303^{0}C is observed due to the conversion of ortho-phosphoric acid in to meta-phosphoric acid, which is ideally occurring at 316 ^{0} C, by removal of two water molecules occurring between 245^{0}C to 600^{0}C. And the final decomposition occurs by removal of one water molecule and meta-phosphoric acid gets converted in to the residual product, i.e. , phosphorus pentoxide , which starts evaporating (sublimation) at 755^{0}C, showing small endothermic peak. The broad exothermic reaction at 650^{0}C represents the reaction occurring in the gas phase during heavy decomposition.

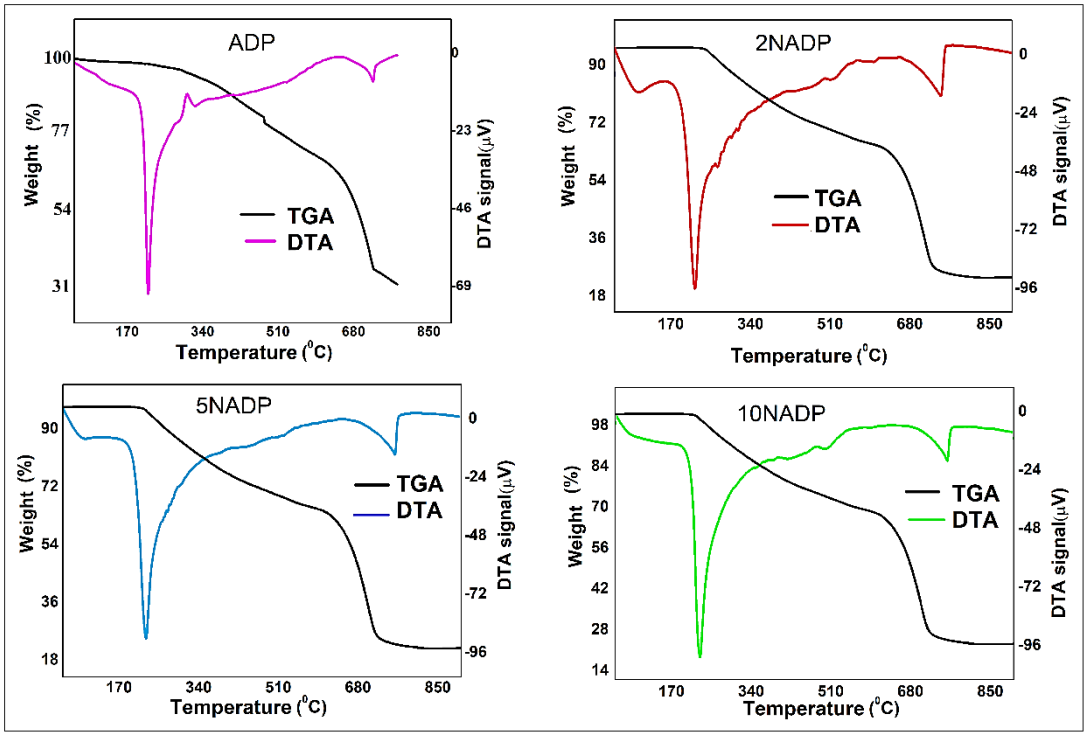


Figure (8): Thermograms of pure and Na_2S added ADP

Table 3: Theoretical and Experimental weight percent values and chemical reactions for pure ADP

Temperature (^{0}C)	Reactions Involved	Weight (%) Theoretical	Weight (%) Experimental
50-150	No decomposition	100	100
150-245	$2NH_4H_2PO_4 \rightarrow 2NH_3+2H_3PO_4$	95	94.3
245-600	$2H_3PO_4 \rightarrow 2H_2O+2HPO_3$	68	68.6
600-780	$2HPO_3 \rightarrow H_2O+P_2O_5$	35	35.6

However, in the Na_2S added ADP crystals, thermal stability marginally decreases and remains stable up to 173^{0}C. It is important to note that the thermal analysis is carried out in atmosphere of air. From table 3, one can find that the three processes occurring in the pure

ISSN: 3139-0951 (Online)
Vol 2/Issue1/ January--June/2026

ADP sample. Here, the thermal stability of Na_2S added ADP is less stable compared to pure ADP. The reason may be that the possible formation of di-ammonium sulphide may invite thermal decomposition slightly early in Na_2S added ADP. It is important to note that di-ammonium sulphide decomposes at ambient conditions.

Dielectric study:

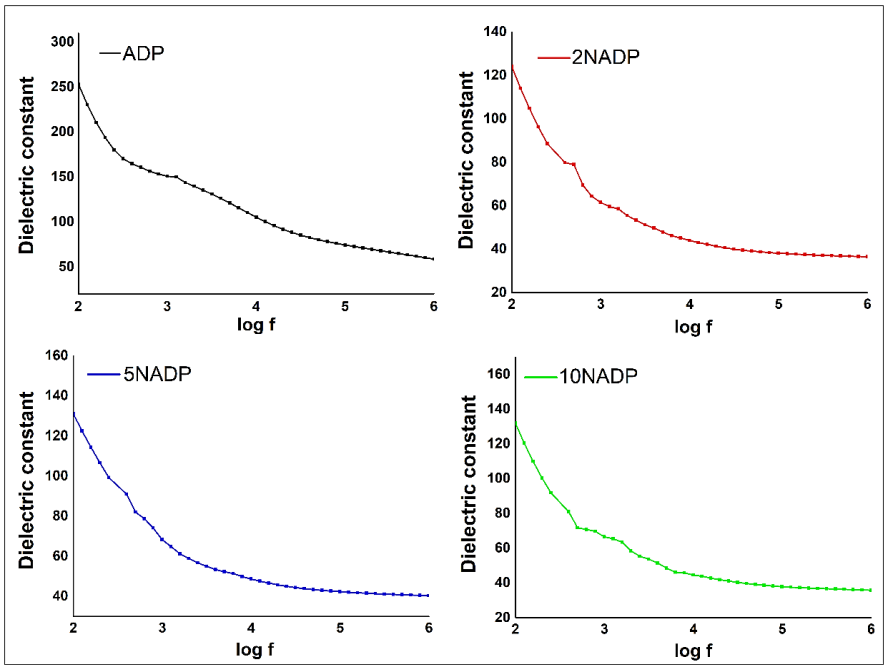


Figure (9): Dielectric constant versus log f of pure and Na_2S added ADP crystals

Figure (9) shows variations of dielectric constant with respect to logarithm of frequency of applied field for pure and Na_2S added ADP crystals. Higher dielectric constant values at lower frequency for all the samples is due to the contribution of all kinds of polarizations, Viz., electronic, ionic, orientation and space charge polarizations. As the frequency increases, the dielectric constant decreases because the dipoles cannot comply with the variation of the external field and hence the polarization decreases. The doped samples possess low dielectric constant compared to pure ADP crystal. This is further explained in detail in Chapter IV. Figure (10) shows variation in dielectric loss with respect to frequency. From the figure, it can be seen that the doped samples exhibit less dielectric loss compared to pure ADP, which indicates that the doped samples possess minimum defect and good optical properties [20].

The a.c. conductivity is calculated using the following formula:

ac conductivity,

$$\sigma_{ac} = \frac{2\pi f C \varepsilon'' t}{A} \quad \ldots(1)$$

Where, f is the frequency, C is the capacitance, ε'' is the dielectric loss, t is the thickness of the pellet and A is the cross-sectional area of the pellet. The figure (11) shows the variation of AC conductivity versus *log f* for pure ADP and Na_2S added ADP crystals.

The AC conductivity values are comparatively low in 2NADP, 5NADP and 10NADP crystals of Na_2S added ADP than in pure ADP. This may be due to development of increased partial substitution of sodium ion in ADP impeding the charge carrier motion.

ISSN: 3139-0951 (Online)
Vol 2/Issue1/ January--June/2026

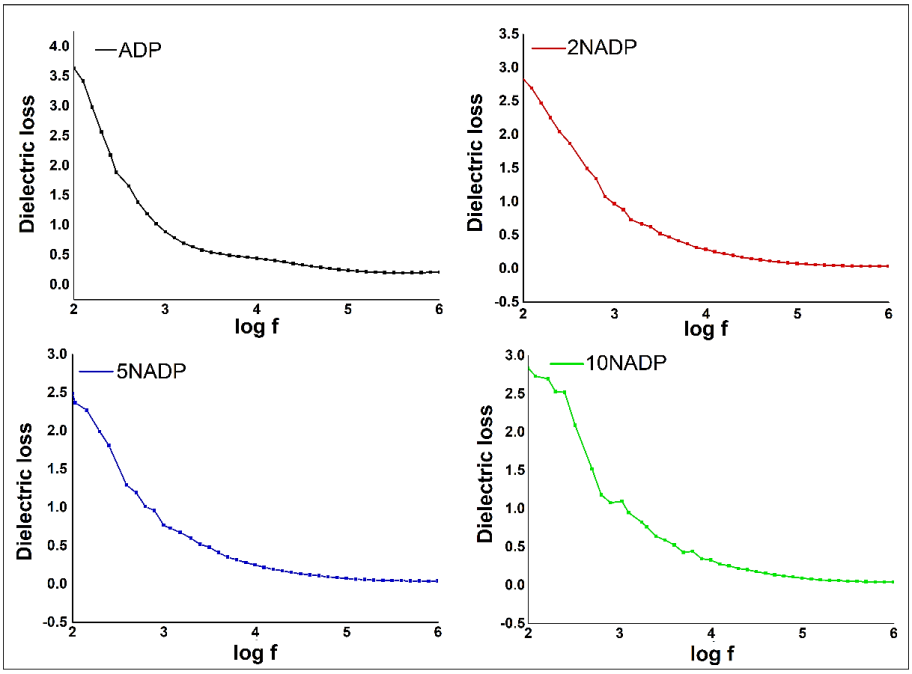


Figure (10): Dielectric loss versus log f for pure and Na_2S added ADP crystals

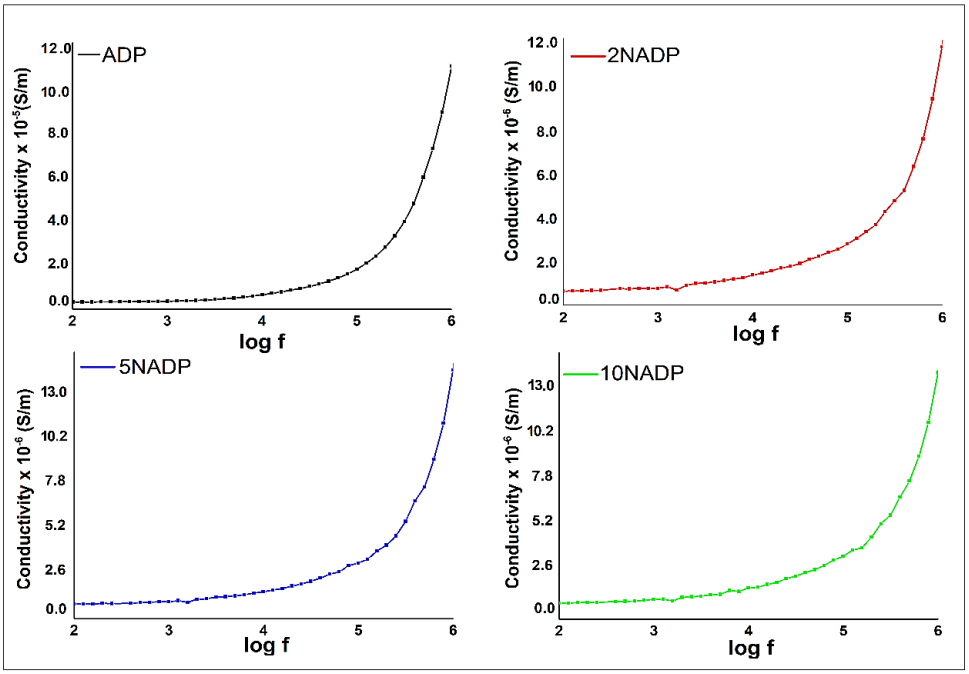


Figure (11): AC conductivity versus log f for pure and Na_2S added ADP crystals

ISSN: 3139-0951 (Online)
Vol 2/Issue1/ January--June/2026

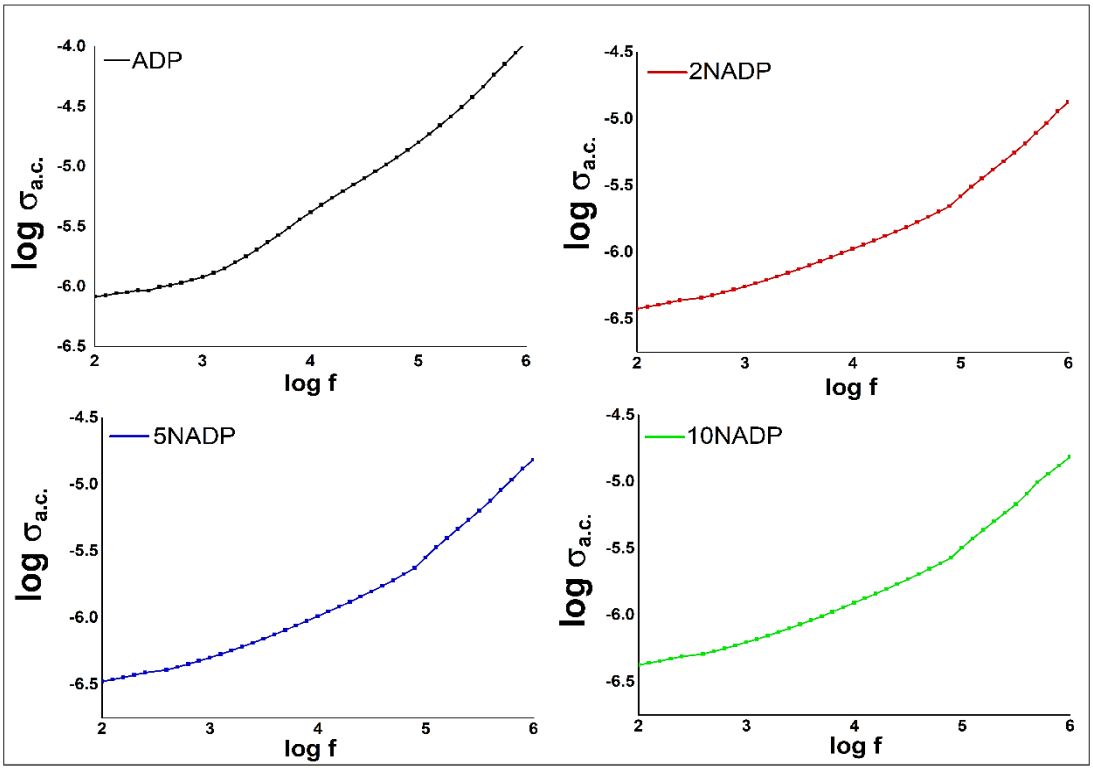


Figure (12): Jonhscher's plots for pure and Na_2S added ADP crystals

Table 4: Parameters from Jonscher's power law

Sample	*n*	*A* (S.m^{-1}.rad^{-n})
ADP	0.71	8.26x10^{-6}
2NADP	0.51	1.58x10^{-8}
5NADP	0.50	1.62x10^{-8}
10NADP	0.47	2.51x10^{-8}

Figure (12) shows Jonscher's plots of both pure and Na_2S added ADP crystals. Jonscher's power law is given by,

$$\sigma_{tot} = \sigma_{dc} + A\omega^n \quad \ldots (2)$$

Where *A* is dependent on temperature and indicates the strength of polarizibility and exponent *n* is the degree of interaction of mobile ions with lattice. Table 4 shows the parameters of Jonscher's plot in which the value of *n* is between 1 and 0.5 which suggests that all the samples possess the ideal long range and diffusion limited hopping. The AC conductivity value is lower for all Na_2S added ADP crystals as compared to pure ADP. The AC conductivity decreases slightly with increase in the doping concentration. The main reason for conduction is due to L-defect (the hydrogen vacancy) in intra-bond jump of proton generates the vacancy and D-defect (double hydrogen bond) at inter-bond jump to a double occupied bond [21].

The electric conduction in ADP is ionic and the migrating charge carrier is proton, which moves in the three-dimensional hydrogen bond network, affecting the motion of neighbouring protons. To occupy the Na_2S molecule in site, it creates a defect. As seen in the receding section that the partial substitution of ammonium by sodium ion generates di-ammonium sulphide. As the conduction in ADP is protonic and mainly due to the anion $[(H_2PO_4)^-]$ and not due to the cation $[(NH_4)^+]$, the partial substitution of sodium ion may increase the defect and as a result, it obstructs the effective of motion of proton. Usually, in case of ionic conductors, the value of *n* can lie between 1 and 0.5 indicating the ideal long-range pathways and diffusion- limited hopping [8]. Here, it was found that the value of degree of correlation of lattice with mobile ions (*n*) lies between 1 and 0.5 suggesting the ideal long-

ISSN: 3139-0951 (Online)
Vol 2/Issue1/ January--June/2026

range pathways and diffusion- limited hopping. The values of *A* and *n* are listed in table 4.

Impedance spectroscopy:

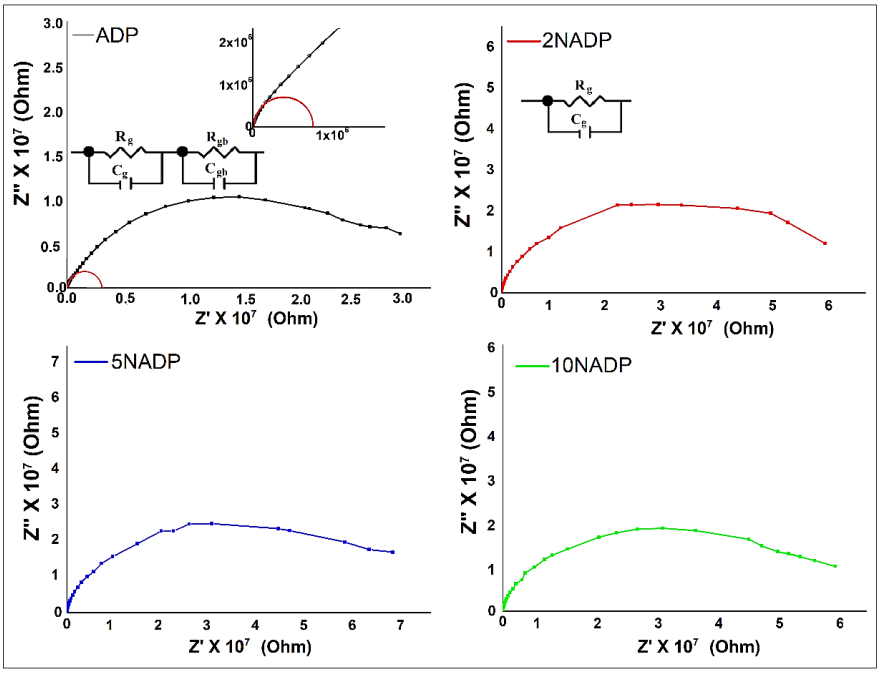


Figure (13): Nyquist plots for pure and Na_2S added ADP crystals

The imaginary and real parts of impedance were obtained from the instrument and plotted with help of software z-view. Figure (13) shows Nyquist plots of pure ADP and Na_2S added ADP crystals. The Nyquist plot is drawn *Z''* versus *Z'* and the higher frequency region is depicted in the plot near to the origin and the low frequency region is represented by the portion away from the origin. The grain and grain boundary contributions can be modelled by equivalent circuit diagram [22]. In the present study, the Nyquist plots are drawn and equivalent circuits are proposed by using the software Z-view. The values of different components for grain and grain boundary are evaluated using the same software. The small semi-circle near the origin for pure ADP at higher frequency region indicates the grain effect and the large semi-circle at lower frequency region indicates the grain boundary effect, while the same plots for the Na_2S added ADP samples show only single semi-circle which indicates grain effect only, within the frequency range studied. The inset figure (13 a) represents the fitted curve in the high frequency region near the origin. The equivalent R-C parallel circuits are presented at inset of figure (13).

Modulus spectroscopy:

To discriminate the electrode polarization and grain boundary effect, complex electric modulus plot is drawn [23–26]. Figure (14) shows complex modulus plots for pure and Na_2S added ADP crystals. In the plot of pure ADP, two clear semi-circles appear due to grain at higher frequency and grain boundary effect at lower frequency, while for the doped ADP crystals, only single semicircle is observed confirming the presence of grain effect only, within the frequency range studied. This study further confirms the results obtained by the Nyquist plots.

ISSN: 3139-0951 (Online)
Vol 2/Issue1/ January--June/2026

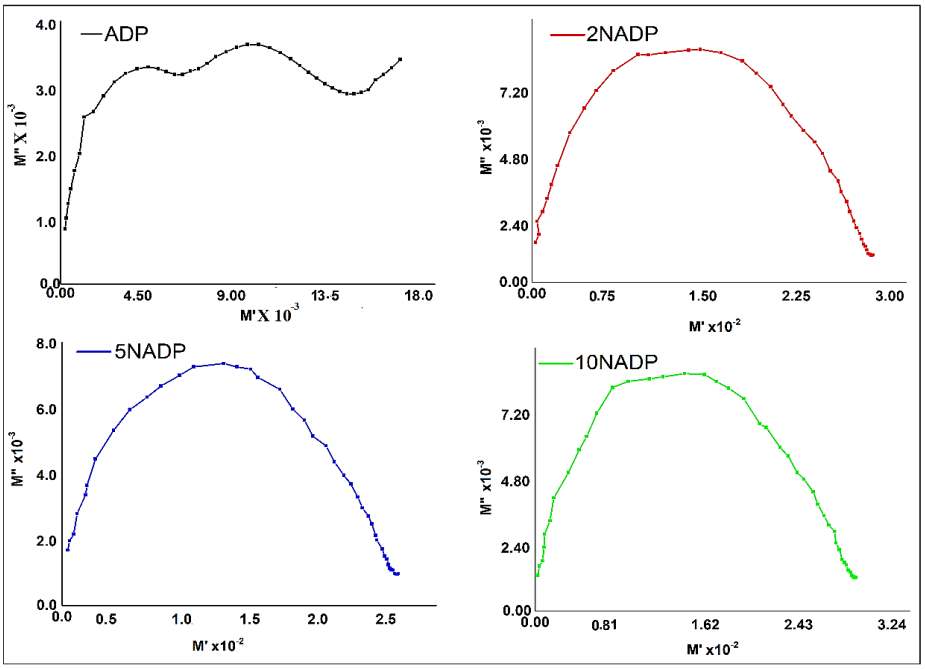


Figure (14): Complex modulus plots for pure and Na_2S added ADP crystals

Table 5: Grain and grain boundary R and C values, Relaxation time and stretch exponent values

Sample	R_g (MΩ)	C_g (pF)	R_{gb} (MΩ)	C_{gb} (pF)	τ_g (mS)	τ_{gb} (mS)	β_g	β_{gb}
ADP	28.9	141.5	30.75	58.47	4.08	1.79	0.145	0.124
2NADP	66.97	43.07	-	-	2.88	-	0.517	-
5NADP	98.28	18.44	-	-	1.81	-	0.520	-
10NADP	48.83	38.32	-	-	1.87	-	0.499	-

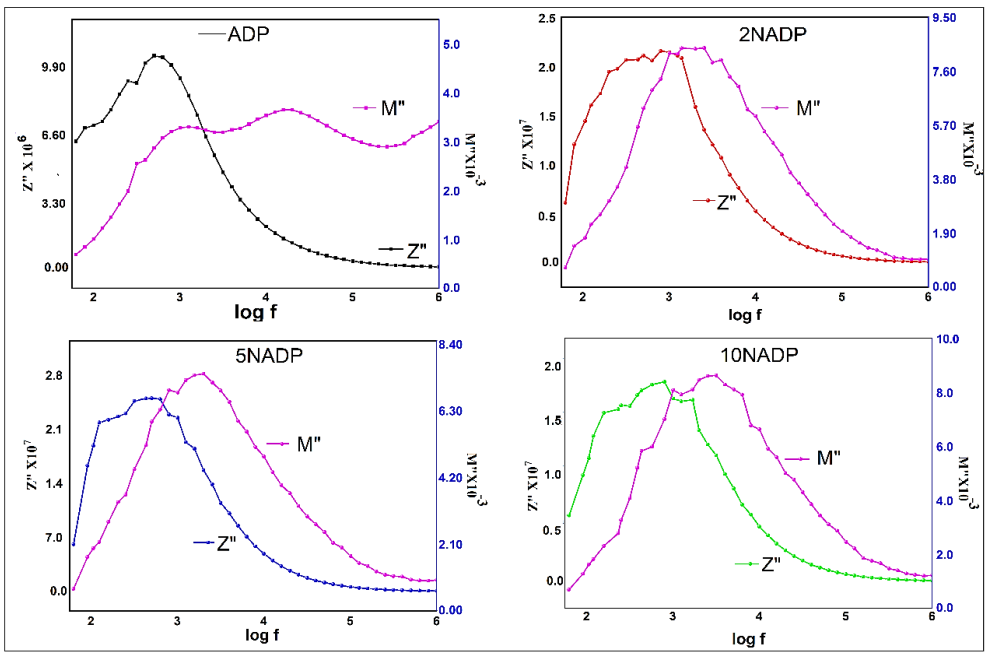


Figure (15): Plots *Z", M"* versus *log f* for pure and Na_2S added ADP crystals

ISSN: 3139-0951 (Online)
Vol 2/Issue1/ January--June/2026

Figure (15) shows the plots of M'' and Z'' versus applied frequency. The modulus spectra of pure and Na_2S added ADP crystals, exhibit broad and asymmetric nature indicating non-Debye type relaxation process with distributed relaxation times about mean relaxation time. The distribution of such relaxation time can be determined by the stretched exponent parameter β, $\beta = \frac{1.196}{W} - 0.047$ $(0 \leq \beta \leq 1)$, where W is FWHM from the M'' versus $log\ f$ plot. The smaller the value of β, the greater is the deviation with respect to Debye type relaxation. The β value is always less than unity for a system in which the dipole-dipole interaction is significant [27]. The above graphs indicate crystal formation.

From table no. 5, it can be seen that the β parameter of doped samples approaches to higher value compared with pure ADP indicates more Debye type relaxation behaviour in doped samples compared to pure ADP. The values of β are given in table 5 and it is found that the Na_2S added ADP crystals exhibit non-Debye type relaxation.

The theoretical correlation between the electro-optic coefficient (r_{eff}) and the dielectric constant for ADP type nonlinear material can be written as [28],

$$r_{eff} = \left\{ \frac{\varepsilon_0 (P-O)}{Ne_c *} \left(\frac{\sum \alpha_1 \alpha_2 \alpha_3}{\sum \alpha_2} \right) f \right\} \left\{ \frac{\varepsilon'_{dc} - \varepsilon'_{\infty}}{\varepsilon'^{\,2}_{\infty}} \right\} \quad \ldots (3)$$

Where, first term = constant =2.47 x 10^{-12}, ε'_{dc} = Relative dielectric constant and ε'_{∞} = Relativity permittivity. When an electric field is applied to a crystal, it causes a change in the anisotropy. The nonlinear electro – optic effect is originated due to two reasons: (i) the lattice ions are displaced by the applied field, thereby changing the electronic susceptibility and (ii) the displacement of electrons within an ions [28]. The values of electro-optic co-efficient of pure and Na_2S added ADP crystals are shown in table 6. The sample 5NADP shows the highest value of electro-optic coefficient.

As ADP is an NLO material, one can predict theoretically the second harmonic generation efficiency (SHG) from the polarizability value using the Clausius-Mosotti equation as given below,

$$\alpha = \frac{3M}{4\pi N\rho} \left[\frac{\varepsilon_{\infty} - 1}{\varepsilon_{\infty} + 2} \right] \quad \ldots (4)$$

Where, α = Polarizability, N = Avogadro number, ε_{∞} = Dielectric constant, M = Molecular mass and ρ = Density. The polarizability values of pure and Na_2S added ADP crystals are tabulated in table 6 at frequency of 10K Hz. Again sample 5NADP shows the highest value of polarizability.

Table 6: Theoretical values of electro-optic and polarizability at frequency of 10K Hz

Sample	Dielectric constant	r_{eff} (pm/V)	α X 10^{-24} (cm^3)
ADP	78.14	2.17	2.4
2NADP	38.84	2.11	2.35
5NADP	43.00	3.47	2.37
10NADP	38.63	2.19	2.35

SHG efficiency by Kurtz Perry method:

The SHG efficiency data are given in table 7 showing the measured SHG values of Na_2S added ADP and the same has been compared with the pure ADP and standard KDP. The SHG efficiency is found to increase for all Na_2S added ADP crystal compared to the pure ADP and KDP.

ISSN: 3139-0951 (Online)
Vol 2/Issue1/ January--June/2026

Table 7: SHG values for pure and Na_2S added ADP crystal

Sample	Output power (mW)	Efficiency	
		Compared to pure ADP	Compared to pure KDP
KDP	14	-	1
ADP	52.5	1.00	3.75
2NADP	105	2.00	7.50
5NADP	130.5	2.48	9.32
10NADP	70.2	1.36	5.01

From table 6 and 7 one can find that the sample 5NADP has highest values of SHG, electro-optic coefficient and polarizability and found to be the superior amongst all samples. Numerous studies on hydrogen bonds such as O-H-O, N-H-O in KDP and ADP had been carried out [29]. It has been found from the second order NLO behaviour of crystals that the hydrogen bonds play a very important role in the NLO contributions to the total nonlinearity. Moreover, the effects of hydrogen bonds in the ADP crystallographic frame and on its optical properties, such as, static polarizability and first hyper polarizability are studied by quantum chemical calculations [30]. The addition of Na_2S is expected to modify the hydrogen bonding PO_4 functional group, which is expected to modify and enhance the SHG efficiency.

Conclusion:

i. The pure and Na_2S added ADP crystals were successfully grown by slow solvent evaporation method. To increase the solubility of chalcogenide compound Na_2S in water the synthesized nanoparticles of Na_2S were used for addition in ADP solution.

ii. The powder XRD study suggests tetragonal crystal structure of pure and Na_2S added ADP crystals and possessed the single phase nature. Also the marginal lattice strain caused by the dopant was estimated.

iii. The AAS confirmed the presence of Na^+ in Na_2S added ADP. The FTIR spectra confirmed the presence of various functional group such as O-H stretching, P-O-H stretching, PO_4 stretching, etc. The shifting in the various absorption peaks indicated the presence of dopants. The S-H asymmetric vibration absorption peak occurring only in the Na_2S added samples confirmed the presence of sulphur in the samples.

iv. Thermal study of grown crystals was studied by TGA/DTA analysis. The pure ADP crystal remained thermally stable up to 180^0C, whereas the Na_2S added ADP crystals remained thermally stable up to 173^0C. Thermal stability of Na_2S added ADP decreased slightly compared to pure ADP crystal.

v. The dielectric constant and dielectric loss decreased as the frequency increased. The a.c. conductivity drastically changed with frequency beyond 40KHz. Dielectric constant and dielectric loss found to be lower in Na_2S added ADP compared to pure ADP. The Jonscher's law is applied to the a.c. conductivity and various parameters were evaluated.

vi. The Nyquist and complex modulus plots show two semi-circles for pure ADP due to presence of grain and grain boundary contribution and single semi-circle for Na_2S added ADP due to effect of grain only within the frequency range studied. The equivalent RC circuits were proposed for the grain and grain boundary contributions. The R and C values were calculated. All grown crystal possessed non-Debye type relaxation.

vii. The electro-optic coefficients were calculated for pure and Na_2S added ADP crystals. The polarizability values were calculated using Claussis-Mossoti equation. The sample 5NADP exhibited highest values of electro-optic coefficient and polarizability.

ISSN: 3139-0951 (Online)
Vol 2/Issue1/ January--June/2026

viii. The Kurtz powder SHG efficiency was found to be improved by adding Na_2S in ADP crystals compared to pure ADP.

ix. From SHG, electro-optic coefficient and polarizability data it was found that the sample 5NADP was superior to all other samples.

References

[1] I. Chang, Tunable acousto-optic filters: an overview, in: Acousto-Optics: Device Development/Instrumentation/Applications, International Society for Optics and Photonics, 1976: pp. 12–23.

[2] S. Musikant, Optical materials. An introduction to selection and application, Optical Engineering, New York: Dekker, 1985. (1985).

[3] T. Narasimhamurty, T.S., Electro-Optic Effects in Crystals: Pockels Linear Electro-Optic and Kerr Quadratic Electro-Optic Effects, in: Photoelastic and Electro-Optic Properties of Crystals, Springer, 1981: pp. 345–419.

[4] G. gilli, P. Gilli, The nature of the hydrogen bond: outline of a comprehensive hydrogen bond theory, in: The Nature of the Hydrogen Bond, Oxford University Press, 2009.

[5] V.G. Dmitriev, G.G. Gurzadyan, D.N. Nikogosyan, Handbook of nonlinear optical crystals, Springer, 2013.

[6] I.P. Kaminow, An Introduction to Electrooptic Devices: Selected Reprints and Introductory Text By, academic press, 2013.

[7] J. Wei, J. Shen, X. Zhang, S. Guo, J. Pan, X. Hou, H. Zhang, L. Wang, B. Feng, Simple one-step synthesis of water-soluble fluorescent carbon dots derived from paper ash, RSC Advances. 3 (2013) 13119–13122.

[8] J. Joshi, D. Kanchan, H. Jethva, M. Joshi, K. Parikh, Dielectric relaxation, protonic defect, conductivity mechanisms, complex impedance and modulus spectroscopic studies of pure and L-threonine-doped ammonium dihydrogen phosphate, Ionics. 24 (2018) 1995–2016.

[9] J. Joshi, G. Joshi, M. Joshi, K. Parikh, Complex impedance, FT-Raman, and photoluminescence spectroscopic studies of pure and L-phenylalanine doped ammonium dihydrogen phosphate single crystals: the correlation with hydrogen bonding defect, Ionics. (2019) 1–23.

[10] J. Joshi, S. Kalainathan, D. Kanchan, M. Joshi, K. Parikh, Effect of L-threonine on growth and properties of ammonium dihydrogen phosphate crystal, Arabian Journal of Chemistry. (2017).

[11] J. Joshi, S. Kalainathan, D. Kanchan, M. Joshi, K. Parikh, Crystal growth, AC electrical and nonlinear optical studies of pure and dl-methionine doped ammonium dihydrogen phosphate single crystals, Journal of Materials Science: Materials in Electronics. 30 (2019) 2985–2993.

[12] K. Parikh, J. Joshi, M. Joshi, Influence of organic dopants (L-alanine and L-arginine) on structural, spectroscopic and thermal properties of ammonium dihydrogen phosphate crystal, Materials Science-Poland. 35 (2017) 632–638.

[13] J.H. Joshi, K.P. Dixit, K.D. Parikh, H.O. Jethva, D.K. Kanchan, S. Kalainathan, M.J. Joshi, Effect of Sr2+ on growth and properties of ammonium dihydrogen phosphate single crystal, J Mater Sci: Mater Electron. 29 (2018) 5837–5852.

[14] M.J. Joshi, A brief overview on robust nonlinear optical (NLO) crystals KDP and ADP and their doped systems, Asian Journal of Physics. (2018).

[15] C.K.M. J. H. Anitha, C.M. Padma, Effect of ZnS as an impurity on the physical properties of $(NH_4)H_2PO_4$ single crystals, Int. J. Eng. Res. Technol., 10(2013)135.

[16] J.A. Hudson, C. Mahadevan, C. Padma, Growth and characterizations of ADP single crystals added with CdS, Int. J. Eng. Res. Appl. 4 (2014) 257–266.

[17] A. Kochuparampil, J. Joshi, M. Joshi, Growth, structural, spectroscopic, thermal, dielectric and optical study of cobalt sulphide-doped ADP crystals, Modern Physics Letters B. 31 (2017) 1750246.

[18] P. Dhanaraj, N. Rajesh, Effect of Amino Acid Additives on Crystal Growth Parameters and Properties of Ammonium Dihydrogen Phosphate Crystals, in: Crystallization and Materials Science of

ISSN: 3139-0951 (Online)
Vol 2/Issue1/ January--June/2026

Modern Artificial and Natural Crystals, IntechOpen, 2012.

[19] P. Shenoy, K. Bangera, G. Shivakumar, Growth and thermal studies on pure ADP, KDP and mixed K_{1-x} $(NH_4)_xH_2PO_4$ crystals, Crystal Research and Technology. 45 (2010) 825–829.

[20] D. Zion, S. Devarajan, T. Arunachalam, Dielectric and optical characterization of boron doped ammonium dihydrogen phosphate, Journal of Crystallization Process and Technology. 3 (2013) 5.

[21] M. Meena, C. Mahadevan, Growth and electrical characterization of L-arginine added KDP and ADP single crystals, Crystal Research and Technology: Journal of Experimental and Industrial Crystallography. 43 (2008) 166–172.

[22] M.J. Joshi, Importance of Impedance Spectroscopy Technique in Materials Characterization: A Brief Review, Mechanics, Materials Science & Engineering MMSE Journal. Open Access. 9 (2017).

[23] P. Macedo, The role of ionic diffusion in polarisation in vitreous ionic conductors, Phys. Chem. Glasses. 13 (1972) 171–179.

[24] F. Howell, R. Bose, P. Macedo, C. Moynihan, Electrical relaxation in a glass-forming molten salt, The Journal of Physical Chemistry. 78 (1974) 639–648.

[25] E. Barsoukov, J.R. Macdonald, Impedance spectroscopy: theory, experiment, and applications, John Wiley & Sons, 2018.

[26] N.G. McCrum, B.E. Read, G. Williams, Anelastic and dielectric effects in polymeric solids, (1967).

[27] M. Dasari, K.S. Rao, P.M. Krishna, G.G. Krishna, Barium Strontium Bismuth Niobate Layered Perovskites: Dielectric, Impedance and Electrical Modulus Characteristics., Acta Physica Polonica, A. 119 (2011).

[28] C.-C. Shih, A. Yariv, A theoretical model of the linear electro-optic effect, Journal of Physics C: Solid State Physics. 15 (1982) 825.

[29] D. Xue, S. Zhang, Effect of hydrogen bonds on optical nonlinearities of inorganic crystals, Chemical Physics Letters. 301 (1999) 449–452.

[30] D. Xue, H. Ratajczak, Effect of hydrogen bonds on physical properties of ammonium dihydrogenphosphate crystals, Journal of Molecular Structure: Theochem. 716 (2005) 207–210.